Polymer 77 (2015) 312–322

Contents lists available at ScienceDirect

Polymer

journal homepage: www.elsevier.com/locate/polymer

Full silicone interpenetrating bi-networks with different organic groups attached to the silicon atoms

Codrin Tugui, Maria Cazacu*, Liviu Sacarescu, Adrian Bele, George Stiubianu, Cristian Ursu, Carmen Racles

"Petru Poni" Institute of Macromolecular Chemistry Iasi, Aleea Grigore Ghica Voda 41A, 700487, Romania

ARTICLE INFO

Article history:
Received 6 April 2015
Received in revised form
17 September 2015
Accepted 18 September 2015
Available online 21 September 2015

Keywords:
Silicones
Interpenetrated networks
Dielectric permittivity
Mechanical characteristics

ABSTRACT

Mixed silicone interpenetrating networks have been prepared using two groups of siloxane polymers and copolymers as precursors in different combinations. Each combination chosen, after a good mixing in solution with cross-linking agents was processed into film, which has been stabilized through sequential crosslinking using separate chemical pathways: condensation with tetraethyl orthosilicate at room temperature for the first network and addition (hydrosilylation) at higher temperatures in the case of the second one. The morphology of the resulted materials was studied by scanning electron microscopy (SEM). The mixing degrees of the two networks were estimated on the basis of the differential scanning calorimetry (DSC) traces as well as by small angle X-ray scattering (SAXS). The obtained films were characterized from point of view of the properties of interest for electromechanical applications by mechanical testing, dielectric spectroscopy and electrical breakdown measurements. The influence of the nature and content of the polar groups attached on the silicon on these characteristics was discussed.

1. Introduction

Since they have been discovered, the dielectric elastomers (DE's), show a continuous interest due to the wide field of applications including their use as actuators in biomedical engineering, artificial muscles, haptic screens or for energy harvesting [1,2]. Besides acrylic elastomers, silicones occupy a top position in this research area due to their special properties derived from unique characteristics of the siloxane bond: shortness and large angle, accounted either to (p → d)π back-bonding or to ionic character [3]. These lead to high intramolecular bond energy and flexible polymer chain. The presence of the organic nonpolar groups attached to the silicon atoms, as in PDMS for example, is the reason for weak intermolecular forces [4]. Silicones show a unique flexibility, with shear modulus *G* values between 100 kPa and 3 MPa and loss tangent values, tan σ << 0.001 [5–6]. On the other hand, the tensile strength is higher than for most organic elastomers at elevated temperatures. In addition, silicone elastomers can operate in a wide range of temperature, without being affected by the moisture, are resistant to oxygen, ozone and sunlight irradiation, have a good dielectric strength and no toxicity, which make them suitable for a large number of applications [6–10]. However, as concerning the electromechanical applications, silicones have the disadvantage of a low dielectric permittivity. Therefore, a significant research effort was focused to improve the dielectric permittivity by incorporating various fillers in the polymer matrix or by attaching polar groups to the polymer network [11–25]. However, by these approaches, the mechanical properties of these materials could be damaged [26]. As for most electroelastomers, mechanical prestrain is generally required to obtain high electromechanical strain and high elastic energy density although the prestrain causes a reduction in certain parameters of the actuators. An interesting approach is to create and maintain prestrain by interpenetrating polymer networks (IPNs) [27]. In the literature there are a number of polysiloxane-organic polymers interpenetrated networks, those reported before 2000 being excellently reviewed in Ref. [28] It is highlighted the difficulty of obtaining homogeneous networks due to well-known incompatibility of the silicones with almost any organic component. These silicone-containing networks generally have been found useful as pervaporation membrane in gears, for medical aims (silicone rubber—nylon or PU with trade name Rimplast), in drug release (poly(vinyl alcohol) – polydimethylsiloxane hydrogels), for high temperature damping (polydimethylsiloxane – polyacrylates – polymethacrylates), or sound and vibration

* Corresponding author.
E-mail address: mcazacu@icmpp.ro (M. Cazacu).

http://dx.doi.org/10.1016/j.polymer.2015.09.042
0032-3861/

damping (polysiloxanes - poly(methyl methacrylate)) [29–33]. The use of interpenetrating polymer networks (IPN) as dielectric elastomers is a less addressed attempt to improve both dielectric and mechanical properties [34,35]. Only recently the electroactive interpenetrating networks that to deform easily under the influence of an electric field became of interest. In general, these are constructed by generating a network in the presence of a basic, already formed one [34]. To increase the actuation strain, the primary network is usually prestrained [32]. As electroactive elastomers, IPNs based on VHB and poly(1,6-hexanediol diacrylate) or trimethylolpropane trimethacrylate (TMPTMA) as well as IPNs of silicone and 3M VHB 4910 have been prepared [34–36]. The interpenetrating polymer networks are formed in the highly prestrained VHB acrylic elastomer network [35].

Brochu et al. used a commercial kit consisting in soft room temperature vulcanizing (RTV) silicone as the host elastomer and a more rigid high temperature vulcanizing (HTV) silicone as a guest to prepare IPN. Prestrain was applied to the crosslinked RTV silicone host material, after that the HTV silicone was cured locking the host network in this state [37–39].

Prompted by the Brochu works, our approach consists in the preparation of siloxane–siloxane networks on the basis of several available, in house prepared polymers as network precursors [37]. The two networks differ by the nature of the substituents at the silicon atom, by the molecular masses of the precursors and also by the crosslinking path. Polar groups (phenyl, trifluoropropyl, 3-cyanopropyl) were attached to the silicon belonging to one of the networks in order to increase the dielectric permittivity. In this case, a big challenge is to find a good compatibility between networks, mainly when one network is more polar then the other, because a phase separation may occur. Further, the interpenetration of two networks with high value of dipole moment can lead to a significant decrease of the breakdown strength. The samples were processed as thin films, which have been stabilized through sequential cross-linking using two separate chemical pathways, without prestrain: one is condensation of OH-terminated siloxane copolymers containing various percents of polar groups (phenyl or trifluoropropyl) along the chain and cured by condensation (used as main network), and the second one is addition of α,ω-bis(vinyl)polydimethylsiloxane to α,ω-bis (trimethylsiloxy)poly(dimethylsiloxane-co-methylhydrosiloxane) or α,ω-bis(trimethylsiloxy)poly(methylcyanopropylsiloxane-co-methylhexylsiloxane-co-methylhydrosiloxane)s. The mechanical and dielectric properties, morphology and thermal behaviour of the resulting IPNs were studied.

2. Experimental

2.1. Materials

α,ω-Bis(trimethylsiloxy)poly(methylhydrosiloxane), $M_w = 2200$ g mol^{-1}, octaphenylcyclotetrasiloxane (D_4^{Ph}), ≥98%, n-hexene, octamethylcyclotetrasiloxane (D_4), dibutyltin dilaurate (DBTDL), 95%, and hexachloroplatinic(IV) acid hydrate, ≥99.9% trace metals basis, Sigma–Aldrich, Germany, were used as received. 1,3,5-Trimethyl-1,3,5-tris(3,3,3-trifluoropropyl)cyclotrisiloxane, 97%, tetraethylorthosilicate (TEOS), 99.9%, supplied by Alfa Aesar, Germany were used as such.

Polydimethylsiloxane-α,ω-diol (PDMS) with M_n = 377,300 g mol^{-1}, as determinated by gel permeation chromatography (GPC), was prepared by cationic ring-opening polymerization of octamethylcyclotetrasiloxane (D_4) catalysed by sulphuric acid, according to an already reported procedure [40]. Poly(dimethylsiloxane-co-diphenylsiloxane)-α,ω-diol, PDMDPhS, with $M_n = 104{,}500$ g mol^{-1} was prepared by bulk anionic ring opening copolymerization of the octamethylcyclotetrasiloxane (D_4) and octaphenylcyclotetrasiloxane (D_4^{Ph}), using tetramethylammonium hydroxide as catalyst and a Lewis base (DMF) as promoter, according to procedure described in Ref. [41] The content in phenyl groups estimated on the basis of ^{1}H NMR was 18.4 mol% (Fig. 1).

Poly[dimethylsiloxane-co-methyl(3,3,3-trifluoropropyl) siloxane]-α,ω-diol, PDMTFS, Mn = 64,800 g mol^{-1}, was prepared by ring-opening copolymerization of D_4 with 1,3,5-trimethyl-1,3,5-tris(3,3,3-trifluoropropyl)cyclotrisiloxane in the presence of cation-exchanger, Purolite CT-175. The content of trifluoropropyl groups estimated from ^{1}H NMR spectrum was 15.4 mol% (Fig. 1). The α,ω-bis(trimethylsiloxy)poly(dimethylsiloxane-co-methylhydrosiloxane), PDMMHS, was synthetized by equilibrium copolymerization of D_4 with α,ω-bis(trimethylsiloxy)poly(methylhydrosiloxane) homopolymer in the presence of Purolite CT-175 [40]. The molecular mass of the resulted copolymer determined by GPC was M_n = 17,800 g mol^{-1}. Based on ^{1}H NMR spectrum it has been estimated a content of 19.2 mol% Si–H groups (Fig. 1). This copolymer was used as a precursor to generate Net B, or in general the second networks, by hydrosilylation with another one containing vinyl group (see below Vi_2PDMS). The α,ω-bis(trimethylsiloxy) poly(methylcyanopropylsiloxane-co-methylhexylsiloxane-co-methylhydrosiloxane)s, $PMCyMHS_1$ and $PMCyMHS_2$, with 3-cyanopropyl/hexyl/hydro contents 9.2/82.9/8.9 and 62.1/26.9/11 and Mn = 4600 and 4200, respectively were prepared by co-hydrosilylation reactions of the commercial α,ω-bis(-trimethylsiloxy)poly(methylhydrosiloxane) with found molecular weight Mn of 2200 g mol^{-1}, with allylcyanide and n-hexene [23]. α,ω-Bis(vinyl)polydimethylsiloxane, Vi_2PDMS, was synthesized by an equilibrium cationic ring-opening polymerisation of D_4 in presence of 1,3-bis(vinyl)tetramethyldisiloxane used to block the chains ends [42]. The resulted polymer had $M_n = 40{,}200$ g mol^{-1} as determined by GPC and was used in the addition reaction to achieving the second network of IPN. The percentages of the polar units contained in copolymers were calculated from ^{1}H NMR spectra (Fig. 1).

2.2. Equipments

The Fourier transform infrared (FTIR) spectra were recorded in KBr pellets and ATR mode with Bruker Vertex 70 FTIR instrument, at room temperature. ^{1}H NMR spectra were recorded on a Bruker Avance III 400 MHz spectrometer, using $CDCl_3$ as solvent. The molecular mass of the polymers was determined by gel permeation chromatography (GPC) in $CHCl_3$ on a PL-EMD 950 chromatograph/evaporative mass detector instrument. The morphology of the films was studied by scanning electron microscope (ESEM) type Quanta 200 operating at 20 kV with secondary and backscattering electrons in low vacuum mode. DSC measurements were performed with a DSC 200 F3 Maia (Netzsch, Germany). About 10 mg of sample was heated in pressed and punched aluminium crucibles at a heating rate of 10 °C min^{-1}. Nitrogen was used as inert atmosphere at a flow rate of 100 ml min^{-1}. Small angle X-ray scattering (SAXS) measurements were carried out using a Bruker NanostarU instrument equipped with a X-ray IμS microsource with copper anode and a three-pinhole collimation system. A high sensitive 2D detector, Vantec-2000, having 68 μm resolution was used to record the scattered intensity. The scattered intensity I(q) is measured as a function of the momentum transfer vector $q = 4\pi\sin\theta/\lambda$, where λ is the wavelength of the X-rays (Cu Kα radiation, 1.54 Å), and θ is half the scattering angle. The sample-to-detector distance was 107 cm allowing measurements with q values between 0.008 Å^{-1} and 0.3 Å^{-1}. The angular scale was calibrated by the scattering peaks of a silver behenate standard. The samples to be analysed have been prepared by cutting small square pieces of about 5 × 5 mm of thin

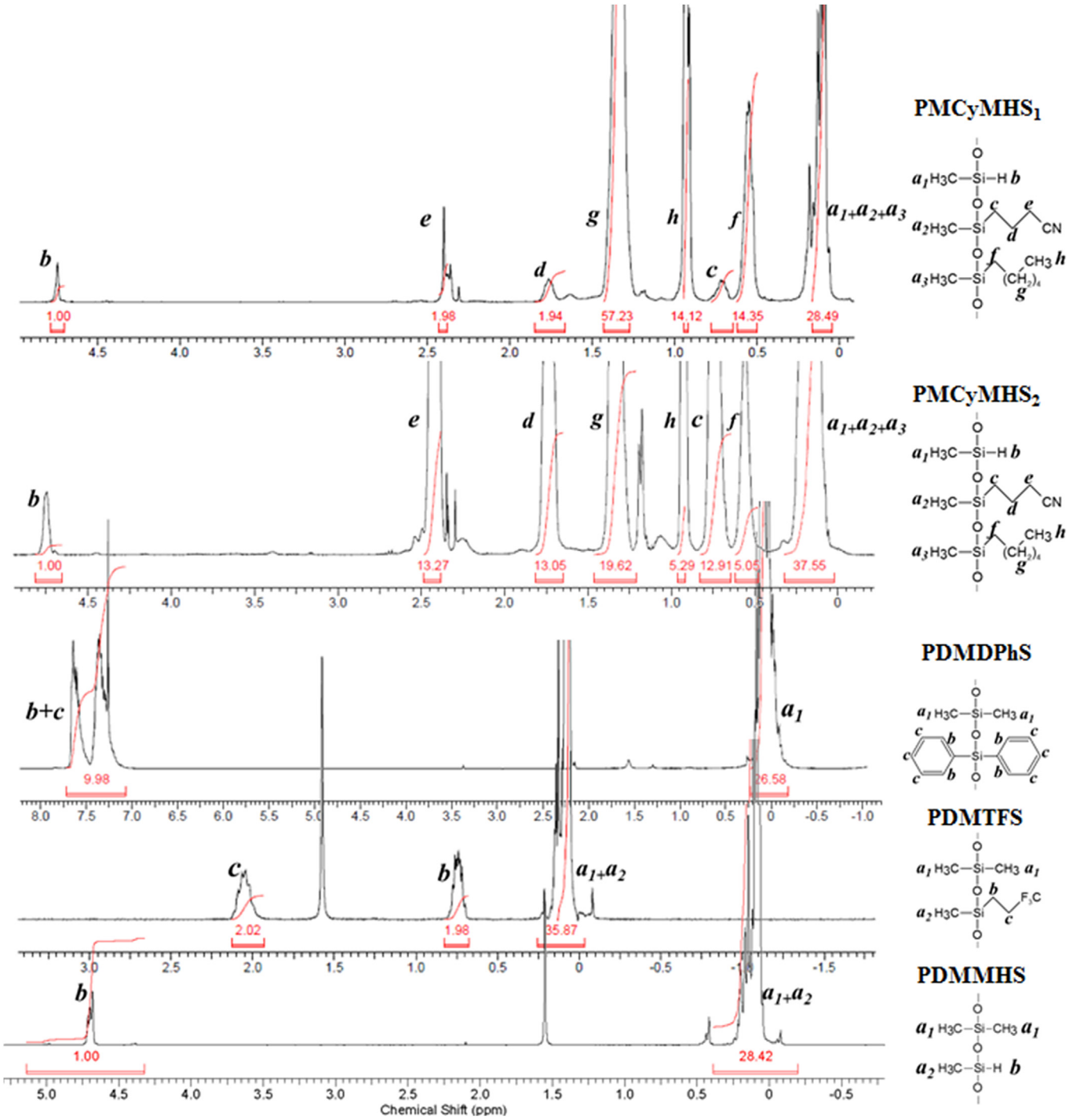

Fig. 1. NMR spectra of precursors for IPNs having different substituents to the silicon atoms: PDMMHS – α,ω-bis(trimethylsiloxy)poly(dimethylsiloxane-co-methylhydrosiloxane); PDMTFS - poly[dimethylsiloxane-co-methyl(3,3,3-trifluoropropyl)siloxane]-α,ω-diol; PDMDPhS - poly(dimethylsiloxane-co-diphenylsiloxane)-α,ω-diol; $PMCyMHS_1$ and $PMCyMHS_2$ – α,ω-bis(trimethylsiloxy)poly(methylcyanopropylsiloxane-co-methylhexylsiloxane-co-methylhydrosiloxane)s.

IPN films, 0.5 mm thick. Then, they were mounted in the dedicated holder and placed inside the sample chamber of the instrument. The IPN samples have been maintained at 25 °C and vacuum for 6 h before starting the measurements. The raw data was normalized for the transmission coefficient and the incoherent scattering due to the background was subtracted in the data analysis using SAXS-NT [43] software. The collected 2D patterns were further reduced by azimuthal integration to 1D plots where the intensity of the scattering, I, is printed versus the momentum transfer vector, q.

Mechanical tests were performed on dumbbell-shaped cut samples from thin films on a TIRA test 2161 apparatus, Maschinenbau GmbH Ravenstein, Germany. Measurements were run at an extension rate of 20 mm min^{-1}, at ambient temperature. To test the fatigue resistance, five cycles were run with: stationary time at maximum strength 5 s, stationary time at minimum strength 5 s, maximum strain 100% and minimum strain 2%. The dielectric

measurements were done with Novocontrol setup (Broadband dielectric spectrometer Concept 40, GmbH Germany) integrating an ALPHA frequency response analyzer and a Quatro temperature control system, with frequency range 10^0–10^6 Hz, at room temperature. The bias voltage applied across the sample was 1.0 V. The samples with uniform thickness were placed between copper plated round electrodes. Breakdown strength measurements were performed in actuation mode, by applying a ramp signal of 400 V s^{-1} on unstressed elastomeric membranes of 22 mm diameter placed between two unequal planar circular electrodes arranged coaxially, as described in Ref. [44] The high voltage electrode dimensions were 25 mm in radius and 25 mm high. The grounded electrode dimensions were 150 mm in radius and 5 mm high. The voltage could vary in the range 0 ÷ 20 kV until the breakdown occurred. Five measurements were made for each sample and the average value was taken into account.

2.3. Procedure for preparing IPNs

All networks were prepared according to the general procedure described below. Thus, 2 g polymer precursor for the first network was dissolved in 20 ml chloroform, and then different amounts of precursors for the second network (Vi_2PDMS and PDMMHS, $PMCyMHS_1$ or $PMCyMHS_2$) were added according to Table 1. After mixing the precursor polymers, 0.16 ml crosslinker (TEOS) and 0.01 ml catalyst (DBTDL) for the first network were added and stirred together. Then, 0.01 ml Speier's catalyst (hexachloroplatinic(IV) acid, 2 wt% solution in isopropanol) was added as a catalyst for the formation of the second network by hydrosilylation and were mixed well. The obtained solutions were drop cast on teflon substrate frames and were left for three days to allow the curing of the first network through a condensation reaction and evaporation of the solvent and by-products. After the first crosslinking was complete, the obtained films, of about 200 μm thickness, were peeled off from substrate and heated at 180 °C for 30 min allowing curing the second network through a hydrosilylation reaction. Before to be tested, the obtained films were aged in normal conditions for two weeks.

3. Results and discussion

For the preparation of the siloxane IPNs, we adapted the procedure described in Ref. [37], according to which two polydimethylsiloxane networks differing by the crosslinking pattern are interpenetrated. Different from this approach, in our work one of the two networks contains different amounts of polar groups attached to the silicon atom: phenyl trifluoropropyl or 3-cyanopropyl. Based on the dipole moment values of the organic groups attached to the silicon atom and estimated by using HyperChem(TM) (0.22, 1.30, 2.85, and 2.92 for $-CH_3$, $-C_6H_5$, $-(CH_2)_2-CF_3$, $-(CH_2)_3-CN$, respectively), the order of the polarity of these groups is: $-(CH_2)_3-CN > -(CH_2)_2-CF_3 > -C_6H_5 > -CH_3$ [45]. In principle, we prepared two networks (Fig. 2): the first one consisting in polydiorganosiloxane-α,ω-diols of high molecular masses (PDMS −377,300 g mol^{-1}, PDMTFS − 64,800 g mol^{-1} or PDMDPhS − 104,500 g mol^{-1}) crosslinked by condensation at room temperature with TEOS. The second one consists in a mixture of α,ω-bis(vinyl)polydimethylsiloxane (Vi_2PDMS) with molecular mass M_n = 40,200 g mol^{-1} and α,ω-bis(trimethylsiloxy)poly(-dimethylsiloxane-co-methylhydrosiloxane) (PDMMHS) with Mn = 17,800 g mol^{-1} and a content of 19.2 mol% Si–H groups or α,ω-bis(trimethylsiloxy)poly(methylcyanopropylsiloxane-co-methylhexylsiloxane-co-methylhydrosiloxane)s, $PMCyMHS_1$ and $PMCyMHS_2$, with molecular masses of 4200 and 4600 and CN-propyl groups content of 62.1 and 9.2 mol%, respectively, in quantities to ensure stoichiometric ratio between Si–CH=CH_2 and Si–H groups (Table 1). These were crosslinked by addition in presence of platinum catalyst. The attempt to crosslink this network in the presence of Karstedt's catalyst failed since the reaction takes place instantaneously not allowing processing of the material in good conditions in the films form. In fact, as demonstrated in a previous publication [46], a dehydrocoupling reaction between Si–H and Si–OH groups (resulted from partial hydrolysis of Si–H in atmosphere) occurs, with formation of SiOSi bond and hydrogen releasing, similar to that proved between Si–H and C–OH with formation of SiOC bond [47]. Therefore, we chose different conditions which allowed better control of crosslinking, i.e. Speier's catalyst and high temperature. No gas releasing was observed in this case.

To get a clear picture of the effects obtained by interpenetration of the two networks as well as by the presence of the polar groups, three reference samples were prepared consisting in two individual networks based on the polymer precursors without polar groups (blank Net A and Net B, respectively) and the derived interpenetrated network (blank IPN-R). The extracts obtained by immersing the samples in THF for 48 h under stirring are between 14.6 and 16.5 wt% (Table 2).

Analysing the extraction behaviour of networks A and B, it can be seen that, as expected, network B crosslinked by hydrosilylation with a ladder pattern shows the smallest soluble fraction, while

Table 1
Recipes used for preparing the IPNs (for first network: crosslinker − 0.16 ml TEOS; catalyst − 0.01 ml DBTDL; for the second network: catalyst − 0.01 ml hexachloroplatinic acid, 2 wt% solution in anhydrous isopropanol).

IPN code	Precursors of the first network				Precursors of the second network						Mol% polar groups in individual network precursor	Mol% polar groups in IPN
	R	R′	Mn	m, [g]	R_1	R_2	Mn $_{Vi2PDMS}$	m $_{Vi2PDMS}$, [g]	Mn_{PDMMHS}/ $Mn_{PMCyMHS^*}$	m_{PDMMHS}/ $m_{PMCyMHS^*}$, [g]		
NetA	CH_3	CH_3	377,300	2	–	–	–	0	–	0	0	0
NetB	–	–	–	0	CH_3	CH_3	40,200	2.71	17,800	0.28	0	0
IPN-R	CH_3	CH_3	377,300	2	CH_3	CH_3	40,200	0.36	17,800	0.04	0	0
IPN-P1	C_6H_5	C_6H_5	104,500	2	CH_3	CH_3	40,200	0.73	17,800	0.07	18.4	12.1
IPN-P2	C_6H_5	C_6H_5	104,500	2	CH_3	CH_3	40,200	0.36	17,800	0.04	18.4	14.6
IPN-F1	$F_3C_3H_4$	CH_3	64,800	2	CH_3	CH_3	40,200	0.73	17,800	0.07	15.4	10.5
IPN-F2	$F_3C_3H_4$	CH_3	64,800	2	CH_3	CH_3	40,200	0.36	17,800	0.04	15.4	12.5
IPN-CN1	CH_3	CH_3	373,000	2	C_3H_4–CN	n-C_6H_{13}	40,200	0.22	4600[a)]	0.15[a]	9.2 (CN)	0.3
IPN-CN2	CH_3	CH_3	373,000	2	C_3H_4–CN	n-C_6H_{13}	40,200	0.26	4200[a)]	0.15[a]	62.1 (CN)	2.4

[a] This was used as an alternative to PDMMHS in the cases of IPN-CN1 and IPN-CN2.

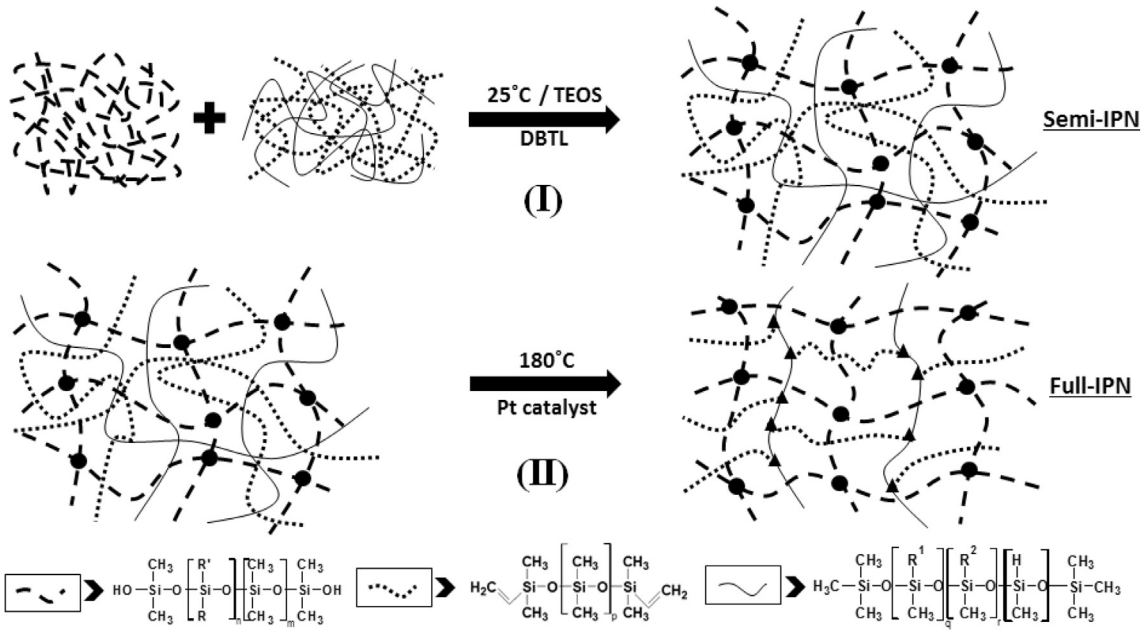

Fig. 2. The sequential pathway to prepare IPN films: **I** – the mixing in solution of the IPN precursors and formation of the first network by crosslinking at room temperature, followed by evaporation of the solvent and condensation by-products; **II** – formation of the second network by hydrosilylation at higher temperature.

network A consisting of a high molecular weight PDMS (377,300) cross-linked by the chain ends as a result of hydrolytic condensation with TEOS shows the highest soluble fraction. Such behaviour of Net A is explicable due to the number of chains in a given mass is small and a single so long uncrosslinked chain that dissolves in the extraction solvent has a high contribution in the extracted masses. In addition, the presence of the macrocycles in high molecular mass PDMS is not excluded. In the case of the IPN-CNs, there may be a suspicion that the involvement of Si–H groups of the copolymer precursors in hydrosilylation reaction would be hampered because of steric hindrance exerted by neighbouring cyanopropyl and hexyl groups and the formation of this network could be compromised [23,48]. However, the soluble fractions in the two networks are within the limits registered for the other networks. The percentage contents of the CN groups in these, estimated on the basis of ^{1}H NMR spectra, although about 10 times higher (3.44 and 24.4 mol% for IPN-CN1 and IPN-CN2 extract, respectively) than in the original samples (0.3 and 2.4 mol% for IPN-CN1 and IPN-CN2, respectively), when reported to the initial sample weight submitted to extraction are actually very small (0.0007 and 0.2530 mol%). The presence of the catalyst (DBTDL) in the extracts is visible both in FTIR (band for ester group at 1732 cm^{-1}) and in ^{1}H NMR spectra (peaks at 1.43, 1.26 and 0.84 ppm). Qualitative information about the content of CN and Si–H groups could also be obtained on the basis of FTIR spectra (Fig. 1S), considering the band at 1263 cm^{-1} assigned to Si–CH$_3$ bond as reference band (Table 3). Considering that one of the networks is mainly composed of chains containing dimethylsiloxane units and the other contains more polar (CN) or less polar (trifluoropropyl, phenyl) groups in different ratios, depending on their nature and distribution pattern along the chain or network, phase separation is possible to occur that could affect both mechanical and dielectric properties [49].

SEM analysis of the cryofractured films reveals a homogeneous structure in the case of blank IPN-R (Fig. 3a), while the images of IPNs having polar groups attached to the silicon atoms, even in lowest content, indicate biphasic morphology of the materials (Fig. 3b,c,d).

To further investigate the phase separation, DSC curves were registered and are presented in Fig. 4. Practically, the glass transition temperature and enthalpy depend on the level of cross-linking, which is affected by the degree of mixing and/or the level of interpenetrating polymer chains. In a phase-separated system, several glass transition temperatures may be registered corresponding to each component. In a homogeneous system, there is a single glass transition, generally ranging between transitions of the components that make up the system [50]. The DSC scans (Fig. 4)

Table 2
The extract obtained after 48 h immersion in THF.

Sample	Extract, [wt%]	Polar group content, mol/ 100 mol SiO units (mol/100 g IPN)		Polar group amount in extract reported to initial IPN, mol/100 mol SiO units (mol/100 g IPN)
		In initial IPN	In THF extract	
Net A	21.4	–	–	–
Net B	3.1	–	–	–
IPN-P1	16.4	n.d.	n.d.	n.d.
IPN-P2	15.8	n.d.	n.d.	n.d.
IPN-F1	14.9	n.d.	n.d.	n.d.
IPN-F2	14.6	n.d.	n.d.	n.d.
IPN-CN1	16.5	0.3 (0.004)	3.4 (0.034)	$0.7\cdot10^{-3}$ ($9.3\cdot10^{-6}$)
IPN-CN2	15.1	2.4 (0.031)	24.4 (0.308)	0.25 (0.003)

n.d. – not determined.

Table 3
The intensity ratios of the representative IR absorption bands for the sample IPN-CN2 as such, extracted in THF for 48 h, as well as for dried extract fraction.

Sample	A_{CN}/A_{1263} [a]	$A_{Si\text{-}H}/A_{1263}$ [b]
Initial	0.065	0.070
Extracted	0.047	0.021
Extract	0.293	0.084

[a] A_{CN}, A_{1263} – absorbance intensity for C≡N (2147 cm^{-1}) and Si–CH_3 (1263 cm^{-1}) bond, respectively.
[b] $A_{Si\text{-}H}$ – absorbance intensity for Si–H bond (2170 cm^{-1}).

revealed for IPN-R, as expected, a single Tg around −123 °C. IPN-P1 also exhibited a single glass transition at −87 °C as a result of the good mixing (presumed by interpenetration) of PDMS with more rigid dimethyldiphenylsiloxane random copolymeric chain.

The samples IPN-F1 and IPN-CN2 show two glass transition pairs, at −119 and −68 °C, and at −124 and −75 °C, respectively, clearly indicating a phase separation, as SEM images also showed. All samples exhibited an endothermal peak at around −40 °C assigned to melting of PDMS [51]. These peaks are not identical in the four types of IPNs, their intensities indicating different crystallization propensity during the cooling of the samples (Table 1S). For example, IPN-F1 exhibited a polymorphic melting, while IPN-CN2 showed a very pronounced melting endotherm, in agreement with the most pronounced phase separation, as a consequence of the largest difference in polarity between the two components.

The IPN films in which there are premises for phase separation, as SEM and DSC analyses already emphasized, were analysed by SAXS. Fig. 5 shows the obtained SAXS curves (plots of the scattered

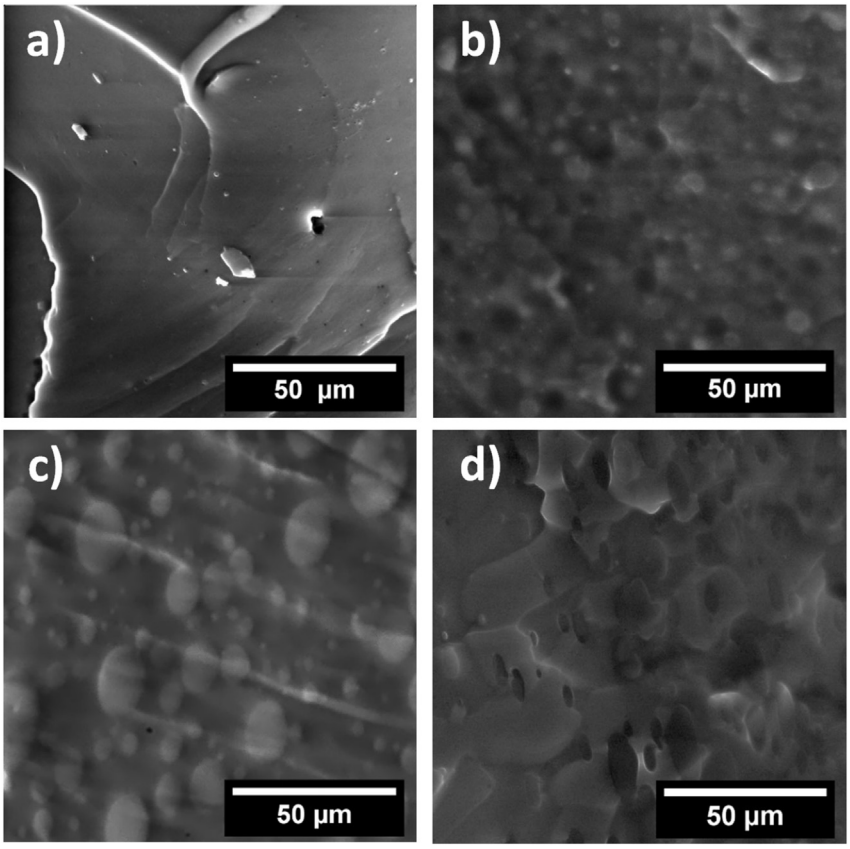

Fig. 3. SEM images of cryo-fractured films: a) IPN-R, b) IPN-P1, c) IPN-F1 and d) IPN-CN2.

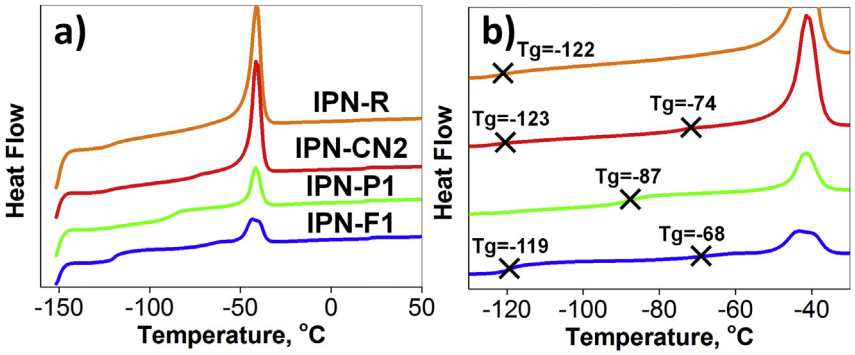

Fig. 4. DSC traces for samples IPN-R, IPN-P1, IPN-F1, IPN-CN2: a) – on the entire temperature range analysed; b) – details emphasizing glass transitions within negative temperature range.

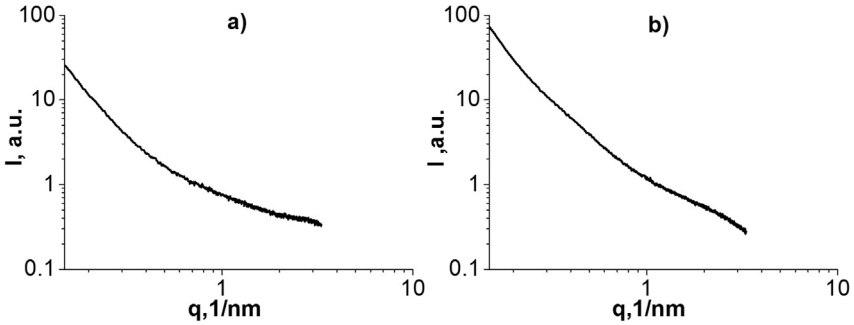

Fig. 5. SAXS curves for the IPNs having the highest percents of most polar groups: a) IPN-F2; b) IPN-CN2.

intensity (I) versus the scattering vector (q) in logarithmic form) for IPN-F2 and IPN-CN2. The samples have the characteristics of typical non-crystalline polymer mixtures. The morphological aspects of the studied IPNs can be revealed by means of the Debye–Bueche method [52–54].

This approach is based on the correlation function theory. The correlation function, g(r), can be obtained by the Fourier transformation of the scattering intensity, I(q). For undefined morphological domains separated at distance r, the correlation function, g(r), is given by the Eq. (1): [55]

$$g(r) = e^{\left(-\frac{r}{a_c}\right)} \tag{1}$$

The coefficient a_c represents the correlation distance defined as the size of an inhomogeneity existent in the sample (Fig. 6).

Since the corresponding scattering intensity could be defined as:

$$\frac{1}{I(q)} = \left[\frac{1}{A} + \left(\frac{a_c^2}{A}\right) \times q^2\right]^2 \tag{2}$$

where A is a constant, then, a_c is easily calculated by plotting $I(q)^{-1/2}$ versus q^2, a graphical approach (Fig. 7) which is known as Debye-Bueche plot: [56]

$$a_c = \frac{\left(\frac{slope}{intercept}\right)^2}{2\pi} \tag{3}$$

The linear part of these plots was used to obtain the short range correlation length, a_c; it has been found 1.71 and 1.39 nm for IPN-F2 and IPN-CN2, respectively. It is accepted that the Debye theory provides a general description of an inhomogeneous system, from which scattering measurements can be used to indicate average electron density and the degree of correlation between two fluctuations as a function of their distance of separation. The calculated correlation lengths show that the size of inhomogeneity is higher in IPN-F2 compared with IPN-CN2. The values are small which suggests that the phase separation and scattered intensity are reduced probably because of the internetwork grafting [57,58]. Such IPNs have a high degree of component mixing. If we consider that the coexistence region between the two polymeric networks is the main cause of the inhomogeneities in the IPNs then it is obvious that a better structuring is observed for IPN-F2.

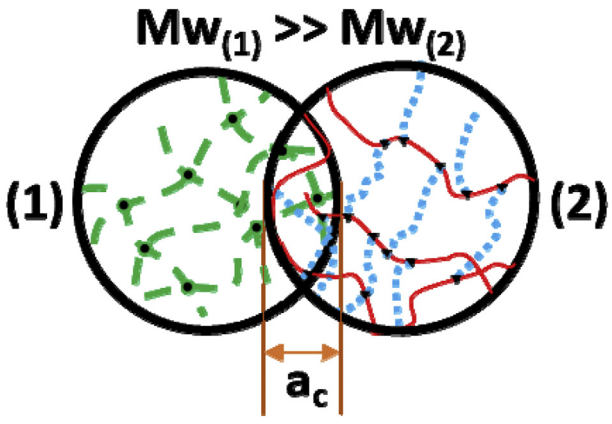

Fig. 6. Schematic representation of the morphological domains and their parameters: (1) – the first network; (2) – the second network; a_c – short range correlation length.

The aged films were investigated from the point of view of the mechanical and dielectric properties.

Stress-strain curves presented in Fig. 8a,b and the data centralized in Table 4 show that the blank IPN-R has an intermediary strain value (484%) as compared with blank samples Net A and Net B, which have elongations of 772% and 262%, respectively. It is presumed that the second network limits the extension of the first network [38].

By interpenetrating the networks containing phenyl or trifluoropropyl groups, a slight decreasing in elongation values as compared with IPN-R sample occurs. When the organic groups from the second networks are cyanpropyl randomized with hexyl ones, as in the samples IPN-CN1 and IPN-CN2, the elongation values are higher, 690 and 518%, respectively. It is presumed that the long hexyl groups have lubrifiant effect allowing easy sliding of chains and networks to each other. Compared to our previously reported interconnected networks [46] and to blends based on PDMS and cyanopropyl-modified silicones [48], the mechanical properties of the IPN-CN samples have been seriously improved. This is on the one hand a positive effect of the IPNs preparation method, and on the other hand, an indirect proof for the formation of interpenetrating networks within the present reaction conditions.

By analysing the data from Table 4, it can be seen that significant decreasing occur in Young modulus values when one of the networks contains polar groups attached. This tendency is more relevant for the samples IPN-Ps and IPN-Fs containing phenyl and trifluoropropyl groups. The cyclic stress-strain curves (Fig. 8c,d) reveal very small hysteresis loops indicating low plastic deformations, this behaviour recommending the IPNs for applications where the samples are subjected to repeated mechanical stress. The value of the applied force appropriate to maximum elongation for each stress-strain cycle, according with the elongation rate, were calculated and plotted in Fig. 9. It can be observed that only small changes appear in the stress relaxation from one cycle to another which demonstrates that the samples show a very small degree of

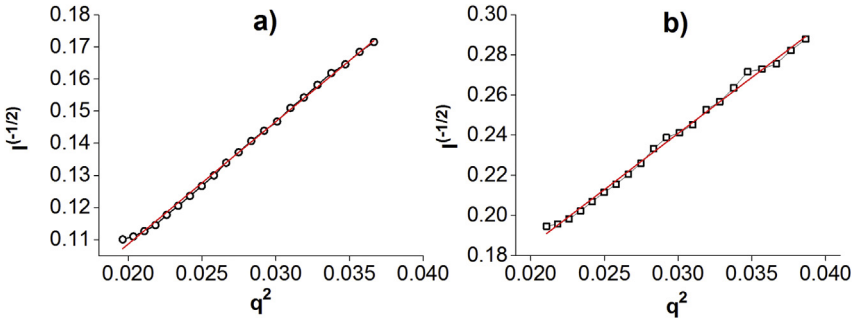

Fig. 7. Linear part of the Debye-Bueche plot for the studied IPNs: a) IPN-F2; b) IPN-CN2.

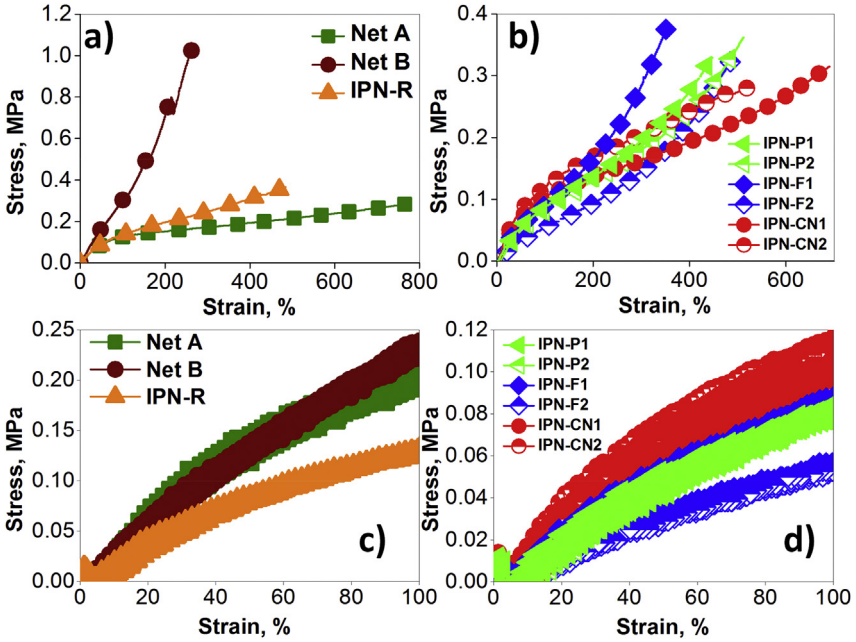

Fig. 8. Mechanical test results: a – stress-strain curves for blank samples Net A, Net B, IPN-R; b – stress-strain curves for new IPNs; c – cyclic stress-strain curves for blank samples Net A, Net B, IPN-R; d – cyclic stress-strain curves for the other IPNs.

relaxation. The region of elastic behaviour for each of prepared materials was estimated as elastic modulus values corresponding to upper limit of this region (Table 4) through the linearization of the first portion of stress-strain curves. Excepting IPN-CN1 and IPN-CN2 samples, which show elastic areas (17 and 16% strains, respectively) almost similar to those of reference networks. The other IPNs show a slight increase of the elasticity domain (19–21%) compared to IPN-R (17%). Also, it can be seen that the limit of elasticity of IPN-R is between the corresponding values of Net A (16%) and Net B (18%). These values are lower than those up to 40% found for RTV 615 from Bayer Silicones and Sylgard 184 from Dow Corning thermally treated 4 h at 200 °C [59].

The permittivity and dielectric losses, as a function of frequency for IPN films containing different polar groups as compared with reference samples are plotted in Fig. 10. By analysing the dielectric permittivity curves, it is clearly observed that although the blank

Table 4
The main mechanical and dielectric characteristics of the prepared IPNs measured at room temperature.

Sample name	Elastic modulus, [MPa[a]]	Young modulus, [MPa[b]]	Elongation, ε, [%]	ε′ at 5 Hz	ε′ at 10^4 Hz	E″ at 5 Hz	ε″ at 10^4 Hz	Breakdown strength, [MV/m]
Net A	1.77	0.20	770	2.97	2.95	0.32	0.0009	>60
Net B	2.32	0.34	262	3.13	3.06	0.24	0.0050	>60
IPN-R	1.72	0.27	484	2.96	2.92	0.56	0.0049	>60
IPN-P1	0.78	0.11	512	3.07	3.01	0.79	0.0041	12
IPN-P2	0.69	0.10	447	3.09	2.97	1.70	0.0007	18
IPN-F1	0.89	0.11	352	8.11	3.70	43.12	0.09714	16
IPN-F2	0.56	0.03	486	5.85	3.62	68.49	0.1073	15
IPN-CN1	0.94	0.13	690	9.27	2.96	10.75	0.0207	29
IPN-CN2	1.25	0.20	518	3.95	3.46	0.98	0.0777	19

[a] Young's modulus at upper limit of the elastic region.
[b] Young's modulus at 10% strain.

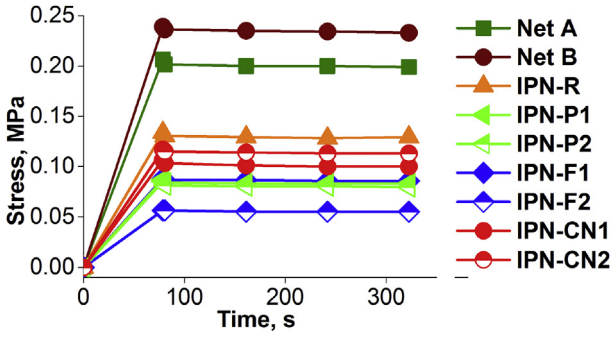

Fig. 9. Stress relaxation for tested samples.

samples have very close values for the dielectric permittivity (2.92–3.06 at 10^4 Hz), a distinction between them can be done (Fig. 10a). Thus, the Net B shows the greatest values of the dielectric permittivity throughout the frequency range. This could be due to crosslinking ladder pattern that reduces the free volume of the network. Net A is crosslinked through chain ends and the sequences between crosslinks are longer thus having a lighter packing and this could lead to lower values of the dielectric permittivity. For IPNs, they decrease from the value corresponding to Net B at 1 Hz to values lower even than those of the Net A at frequencies above 10 Hz and decrease continuously within the studied frequency range. On the other hand, the dielectric permittivity values of the blank samples are maintained almost constant for the entire range of frequency excepting IPN-R where a small increasing in the low frequency range was observed (Fig. 10a). At the same time, it was found an increasing of the dielectric losses for all samples in the low frequency range (Fig. 10c). When polar groups are attached to one of the networks, as can be observed in Fig. 10b and Table 4, dielectric permittivity at low frequencies is significantly higher than for blank IPN, depending on the polarity of the organic groups. The highest value at 5 Hz was recorded for sample IPN-CN1 ($\varepsilon = 9.27$) followed by IPN-F1 ($\varepsilon = 8.11$). As the frequency increases, the permittivity decreases significantly reaching a plateau around 10^3 Hz in all cases, as observed in the case of precursors of the IPN-CNs [23]. In high frequency region, the differences between the values of dielectric permittivity of the analysed samples are not so high, at 10^4 Hz these ranging between 2.96 (IPN-CN1), 2.97 (IPN-P1) and 3.63, 3.70 (IPN-Fs). The dielectric losses at low frequencies are also high reaching values of $\varepsilon'' = 68.49$ and 43.12 in the case of IPN-Fs at 5 Hz. As frequency increases, a significant decrease of dielectric losses occurs tending to zero (Fig. 10d, Table 4).

The breakdown field values reveal a clear decrease with the introduction of polar groups and their content, from >60 MV/m in the cases of the reference samples Net A, Net B and IPN-R to 12–18 MV/m for IPN-Ps and IPN-Fs with a content of polar groups between 10.5 and 14.6 mol%. Although they contain the most polar groups, the IPN-CNs show slightly higher breakdown field values (29 and 19 MV/m) as compared with the previous because their content is very low (0.3 and 2.4 mol%, respectively). The decreasing in breakdown field value as the polarity of the material increases is an expected, well-known behaviour due mainly to large dielectric losses. Failure to entirely dissipate heat generated by these losses, as well as increased amount of moisture absorbed that promotes electrolytic processes could be an explanation for this shortcoming [24]. The values found for IPN-CNs are comparable with those reported by Risse et al. [48] for blends and much lower than those found for interconnected networks with cyanopropyl polar groups [46]. However, the measuring protocol in this case differs from the ones used by other groups [48], i.e. we used a 400 V/s ramp and 22 mm planar electrodes, versus 50 or 100 V/s and spherical electrodes and the measurements were carried out in actuation mode, as it allowed our equipment. The film thickness during actuation diminishes; however, the breakdown is reported to the initial thickness of the film. While a larger electrode area and a greater ramp could give more accurate results in terms of overall material behaviour, the presence of small voids or other defects in the tested materials would clearly limit the breakdown values. Thus, the comparison with similar materials in the literature is rather imprecise.

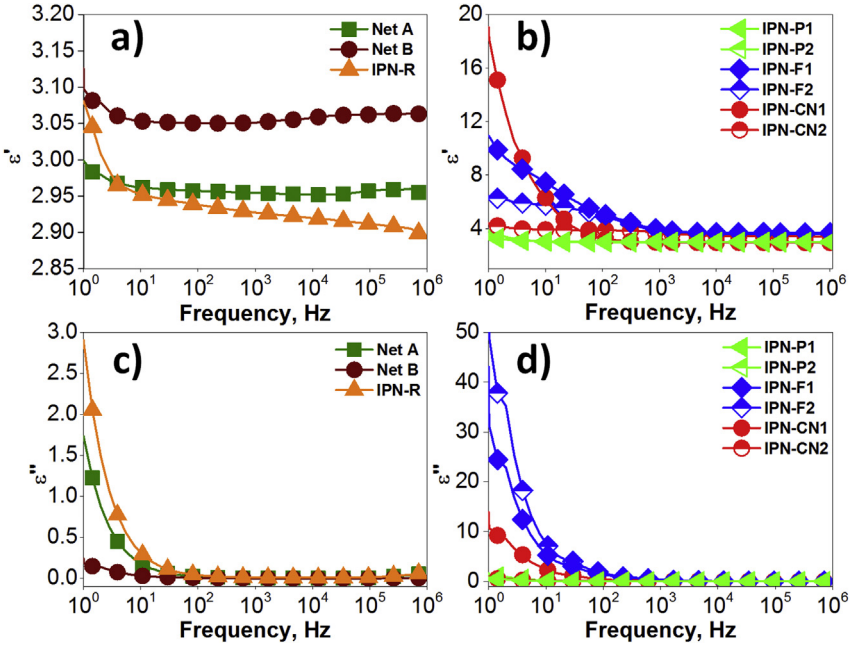

Fig. 10. Dielectric spectra in dependence on frequency: a) dielectric permittivity of blank samples, Net A, Net B, IPN-R; b) dielectric permittivity of IPNs containing different percentages of polar groups, c) dielectric losses of blank samples and d) dielectric losses of IPNs containing different percentages of polar groups.

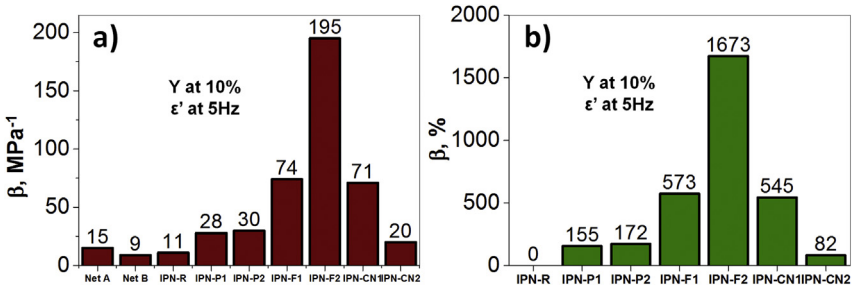

Fig. 11. Comparative graphical representations of electromechanical sensitivity values: a) – absolute values calculated according to ref. [58]; b) – percentage changes in the electromechanical sensitivity of the IPNs as compared with reference IPN-R (β, % = 100 (β_{IPN}- β_{IPN-R})/β_{IPN-R}, where IPN can be any of the networks functionalized with polar groups).

The mechanical and dielectric characteristics can be used to estimate a parameter of interest for future potential application of such materials in electromechanical devices (e.g., actuation or harvesting). Thereby, the electromechanical sensitivity, $\beta = \varepsilon'/Y$, was calculated using the dielectric permittivity (ε') at 5 Hz and the Young's modulus (Y) at 10% strain [60]. Fig. 11 reveals that the highest values, 74 and 195 MPa^{-1}, were obtained for IPN-F1 and IPN-F2 containing high percents (10.5 and 12.5 mol%, respectively) of highly polar trifluoropropyl groups. This means an increase in this parameter with 573 and 1673%, respectively, compared to the reference sample IPN-R (Fig. 11b). These samples showed also the lowest values for Young modulus and highest values for dielectric permittivity (8.11 and 5.85, respectively) at 5 Hz.

4. Conclusions

Interpenetrating polymer networks (IPN) have been achieved based on two silicone systems, one of them containing various percents of trifluoropropyl, phenyl or 3-cyanopropyl groups along the chain. One silicone network consists in OH-terminated siloxane copolymers cured by condensation, while the second one is composed by an α,ω-bis(trimethylsiloxy)poly(dimethylsiloxane-co-methylhydrosiloxane) or α,ω-bis(trimethylsiloxy)poly(-methylcyanopropylsiloxane-co-methylhexylsiloxane-co-methylhydrosiloxane)s by addition with α,ω-bis(vinyl)polydimethylsiloxane. Samples containing siloxane components with polar groups, even in low contents showed phase separation as SEM images and DSC curves revealed. SAXS results confirmed the IPNs structure by the presence of a degree of correlation between two domains as a function of distance of their separation. From mechanical point of view the IPN-CN1 sample showed the best strain (about 700%) as compared with the blank IPN-R. In the same time, all samples have a small mechanical hysteresis when they are subjected to repeated cyclical stress tests. The dielectric results point out that the dielectric permittivity shows a significant increase only in the low frequency range where the dielectric losses are also high as compared with the blank samples but decreasing as frequency increases. At higher frequencies, the effect of the polar groups on the dielectric permittivity is less spectacular. However, the calculated electromechanical sensitivity point towards very promising actuation behaviour for the most polar networks, especially for the ones containing trifluoropropyl or cyanopropyl groups.

Acknowledgements

The work presented in this paper is developed in the context of the project PolyWEC (www.polywec.org, prj. ref. 309139), a FET-Energy project that is partially funded by the 7th Framework Programme of European Community and co-financed by Romanian National Authority for Scientific Research, CNCS-UEFISCDI (Contract 205EU). We also acknowledge the support of Swiss National Science Foundation and UEFISCDI, under the Swiss-Romanian Research Program, grant No. IZERZO_142215/1(10/RO-CH/RSRP/01.01.2013). Thanks to Dr. Stelian Vlad for mechanical measurements as well as to Dr. Cristian Varganici for DSC measurements.

Appendix A. Supplementary data

Supplementary data related to this article can be found at http://dx.doi.org/10.1016/j.polymer.2015.09.042.

References

[1] R. Pelrine, R. Kornbluh, J. Joseph, R. Heydt, Q. Pei, S. Chiba, Mater. Sci. Eng. C 11 (2000) 89.
[2] C. Jean-Mistral, S. Basrour, J.-J. Chaillout, Smart Mater. Struct. 19 (2010) 085012.
[3] H. Oberhammer, J.E. Boggs, J. Am. Chem. Soc. 102 (1980) 7241.
[4] D. Graiver, G. Fearon, in: G. Jones, J.C. Wataru Ando (Eds.), Silicon-Containing Polymers: the Science and Technology of Their Synthesis and Applications, Kluwer Academic Publishers, Dordrecht, 2000, pp. 233–243.
[5] J.A. Clarson, J. Stephen, Semlyen, Siloxane Polymers, Prentisce Hall, 1993, p. 695.
[6] J.C. Lötters, W. Olthuis, P.H. Veltink, P. Bergveld, J. Micromech. Microeng. 7 (1997) 145.
[7] F. Vidal, C. Plesse, G. Palaprat, A. Kheddar, J. Citerin, D. Teyssié, C. Chevrot, Synth. Met. 156 (2006) 1299.
[8] M. Liu, J. Sun, Q. Chen, Sens. Actuators A Phys. 151 (2009) 42.
[9] A. Mata, A.J. Fleischman, S. Roy, Biomed. Microdevices 7 (2005) 281.
[10] Y. Tanaka, K. Morishima, T. Shimizu, A. Kikuchi, M. Yamato, T. Okano, T. Kitamori, Lab. Chip 6 (2006) 230.
[11] J. Chon, S. Ye, K.J. Cha, S.C. Lee, Y.S. Koo, J.H. Jung, Y.K. Kwon, Chem. Mater. 22 (2010) 5445.
[12] S. Nayak, T. Kumar Chaki, D. Khastgir, Adv. Mater. Res. 622–623 (2013) 897.
[13] A.L. Skov, S. Vudayagiri, M. Benslimane, in: Y. Bar-Cohen (Ed.), SPIE Smart Structures and Materials + Nondestructive Evaluation and Health Monitoring, International Society for Optics and Photonics, 2013, p. 86871I.
[14] L.J. Romasanta, P. Leret, L. Casaban, M. Hernández, M.A. de la Rubia, J.F. Fernández, J.M. Kenny, M.A. Lopez-Manchado, R. Verdejo, J. Mater. Chem. 22 (2012) 24705.
[15] H. Liu, L. Zhang, D. Yang, Y. Yu, L. Yao, M. Tian, Soft Mater. 11 (2013) 363.
[16] J. Yang, M. Tian, Q.-X. Jia, J.-H. Shi, L.-Q. Zhang, S.-H. Lim, Z.-Z. Yu, Y.-W. Mai, Acta Mater. 55 (2007) 6372.
[17] M. Cazacu, M. Ignat, C. Racles, M. Cristea, V. Musteata, D. Ovezea, D. Lipcinski, J. Compos. Mater. 48 (2013) 1533.
[18] A. Bele, M. Cazacu, G. Stiubianu, S. Vlad, RSC Adv. 4 (2014) 58522.
[19] A. Bele, M. Cazacu, G. Stiubianu, S. Vlad, M. Ignat, Compos. Part B Eng. 68 (2015) 237.
[20] G. Gallone, F. Carpi, D. De Rossi, G. Levita, A. Marchetti, Mater. Sci. Eng. C 27 (2007) 110.
[21] F. Carpi, G. Gallone, F. Galantini, D. De Rossi, Adv. Funct. Mater. 18 (2008) 235.
[22] C. Racles, M. Cazacu, B. Fischer, D.M. Opris, Smart Mater. Struct. 22 (2013) 104004.
[23] C. Racles, M. Alexandru, A. Bele, V.E. Musteata, M. Cazacu, D.M. Opris, RSC Adv. 4 (2014) 37620.
[24] Z. Ahmad, in: M.A. Silaghi (Ed.), Dielectric Material, InTech, 2012.
[25] M. Misra, M. Agarwal, D.W. Sinkovits, S.K. Kumar, C. Wang, G. Pilania, R. Ramprasad, R.A. Weiss, X. Yuan, T.C.M. Chung, Macromolecules 47 (2014) 1122.
[26] M. Niklaus, H.R. Shea, Acta Mater. 59 (2011) 830.

[27] S.M. Ha, New Electroelastomers for High Performance Actuators, PhD Thesis, Los Angeles, California, ProQuest (2007) 114.
[28] Silicon-Containing Polymers: the Science and Technology of Their Synthesis and Applications 30, Springer Science & Business Media, 2001, p. 768.
[29] B.-Y. Lim, S.-C. Kim, J. Memb. Sci. 209 (2002) 293.
[30] L.H. Sterling, Encycl. Polym. Sci. Technol. 10 (2004) 272.
[31] M.-S. Shin, S.J. Kim, I.Y. Kim, N.G. Kim, C.G. Song, S.I. Kim, J. Appl. Polym. Sci. 85 (2002) 957.
[32] G.-S. Huang, Q. Li, L.-X. Jiang, J. Appl. Polym. Sci. 85 (2002) 545.
[33] N.C. Goulbourne, Int. J. Solids Struct. 48 (2011) 1085.
[34] S.M. Ha, W. Yuan, Q. Pei, R. Pelrine, S. Stanford, Adv. Mater. 18 (2006) 887.
[35] S.M. Ha, W. Yuan, Q. Pei, R. Pelrine, S. Stanford, Smart Mater. Struct. 16 (2007) S280.
[36] S.M. Ha; I.S. Park; M. Wissler; R. Pelrine; S. Stanford; K.J. Kim; G.M. Kovacs; Q. Pei, SPIE proceeding 2008, Proc. SPIE.
[37] P. Brochu, H. Stoyanov, X. Niu, Q. Pei, Smart Mater. Struct. 22 (2013) 055022.
[38] Z. Suo, J. Zhu, Appl. Phys. Lett. 95 (2009), 232909.
[39] S.M. Ha, W. Yuan, Q. Pei, R. Pelrine, S. Stanford, SPIE (2006), 6168.
[40] M. Cazacu, M. Marcu, J. Macromol. Sci. Part A 32 (1995) 1019.
[41] M. Cazacu, A. Vlad, M. Alexandru, P. Budrugeac, C. Racles, F. Iacomi, Polym. Bull. 64 (2009) 421.
[42] M. Cazacu, M. Marcu, A. Vlad, D. Caraiman, C. Racles, Eur. Polym. J. 35 (1999) 1629.
[43] Bruker AXS software.
[44] C. Tugui, G. Stiubianu, M. Iacob, C. Ursu, A. Bele, S. Vlad, M. Cazacu, J. Mater. Chem. C 3 (2015), 8963.
[45] Chemistry Software, HyperChem, Molecular Modeling.
[46] C. Racles, A. Bele, M. Dascalu, V.E. Musteata, C.D. Varganici, D. Ionita, S. Vlad, M. Cazacu, S.J. Dünki, D.M. Opris, RSC Adv. 5 (2015) 58428.
[47] G. Stiubianu, M. Cazacu, A. Nicolescu, V. Hamciuc, S. Vlad, J. Polym. Res. 17 (2010) 837.
[48] S. Risse, B. Kussmaul, H. Krüger, G. Kofod, Adv. Funct. Mater. 22 (2012) 3958.
[49] Y.S. Lipatov, T.T. Alekseeva, Adv. Polym. Sci. 208 (2007) 1. Springer-Verlag, Berlin, Heidelberg.
[50] S.C. Kim, D. Klempner, K.C. Frisch, H.L. Frisch, Macromolecules 9 (1976) 263.
[51] Alex C.M. Kuo, Polymer Data Handbook, 411, 1999.
[52] J.H. An, A.M. Fernandez, L.H. Sperling, Macromolecules 20 (1987) 191.
[53] S. Tan, D. Zhang, E. Zhou, Polym. Int. 42 (1997) 90.
[54] X. Yu, G. Gao, J. Wang, F. Li, X. Tang, Polym. Int. 48 (1999) 805.
[55] P. Debye, H.R. Anderson, H. Brumberger, J. Appl. Phys. 28 (1957) 679.
[56] P. Debye, A.M. Bueche, J. Appl. Phys. 20 (1949) 518.
[57] V. Nevissas, J.M. Widmaier, G.C. Meyer, J. Appl. Polym. Sci. 36 (1988) 1467.
[58] D.J. Hourston, Y. Zia, J. Appl. Polym. Sci. 29 (1984) 629.
[59] F. Schneider, T. Fellner, J. Wilde, U. Wallrabe, J. Micromech. Microeng 18 (2008), 065008 (9pp).
[60] H. Zhao, D.-R. Wang, J.-W. Zha, J. Zhao, Z.-M. Dang, J. Mater. Chem. A 1 (2013) 3140.